Defect studies of ZnO single crystals electrochemically doped with hydrogen

J. Čížek,[1,a)] N. Žaludová,[1] M. Vlach,[1] S. Daniš,[1] J. Kuriplach,[1] I. Procházka,[1] G. Brauer,[2] W. Anwand,[2] D. Grambole,[2] W. Skorupa,[2] R. Gemma,[3] R. Kirchheim,[3] and A. Pundt[3]

[1]*Faculty of Mathematics and Physics, Charles University, Prague, V Holešovičkách 2, CZ-18000 Praha 8, Czech Republic*
[2]*Institut für Ionenstrahlphysik und Materialforschung, Forschungszentrum Dresden-Rossendorf, Postfach 510119, D-01314 Dresden, Germany*
[3]*Institut für Materialphysik, Universität Göttingen, Friedrich-Hund-Platz 1, D-37077, Göttingen, Germany*

Various defect studies of hydrothermally grown (0001) oriented ZnO crystals electrochemically doped with hydrogen are presented. The hydrogen content in the crystals is determined by nuclear reaction analysis and it is found that already 0.3 at. % H exists in chemically bound form in the virgin ZnO crystals. A single positron lifetime of 182 ps is detected in the virgin crystals and attributed to saturated positron trapping at Zn vacancies surrounded by hydrogen atoms. It is demonstrated that a very high amount of hydrogen (up to $\sim$30 at. %) can be introduced into the crystals by electrochemical doping. More than half of this amount is chemically bound, i.e., incorporated into the ZnO crystal lattice. This drastic increase of the hydrogen concentration is of marginal impact on the measured positron lifetime, whereas a contribution of positrons annihilated by electrons belonging to O–H bonds formed in the hydrogen doped crystal is found in coincidence Doppler broadening spectra. The formation of hexagonal shape pyramids on the surface of the hydrogen doped crystals by optical microscopy is observed and discussed. © *2008 American Institute of Physics.* [DOI: 10.1063/1.2844479]

I. INTRODUCTION

ZnO is a wide band gap semiconductor with a variety of applications including UV light emitting diodes and lasers,[1] optoelectronic devices,[2] varistors,[3] and gas sensors.[4] Due to a progress in crystal growth,[5] high quality single crystals are nowadays available. Properties of such ZnO crystals are significantly influenced by lattice defects. A detailed characterization of lattice defects in ZnO crystals is, therefore, a key task in order to understand their physical properties.

In addition to a variety of possible intrinsic defects, complexes of defects with impurities have to be considered as well. Hydrogen is one of the most important impurities in ZnO crystals. It is always present in the crystal growth environment despite of the growth technique used. Density functional theory first principles calculations[6] showed that hydrogen is easily incorporated into the ZnO lattice due to the formation of O–H bonds.

Thus, virgin ZnO crystals may contain a rather high amount of hydrogen. It is desirable to determine the hydrogen content in the ZnO crystals studied and in the case of a significant hydrogen concentration, one has to seriously consider hydrogen interaction with native defects. In the recent work,[7] hydrothermally grown (HTG) and melt grown ZnO crystals from a variety of suppliers were investigated and compared. It was found that all these crystals contain a surprisingly high amount of chemically bound hydrogen.

It is evident that several hydrogen states can be found in a ZnO crystal, namely:

(i) *Hydrogen bound in the lattice*, the calculations[6] revealed that hydrogen occupies the so-called bond-centered (BC) positions. One can distinguish hydrogen in $BC_\parallel$ positions, where the O–H bond is parallel with the c axis, and $BC_\perp$ sites, where it is not parallel. Extended calculations with increased convergence and additional relaxation[8] indicated that the lowest energy sites are $BC_\parallel$ positions. However, the energy difference between the $BC_\parallel$ and $BC_\perp$ is rather small ($\sim$0.1 eV). In agreement with the theoretical prediction, Lavrov *et al.*[8] found a line at 3611 cm^{-1} in infrared (IR) spectra of ZnO crystals treated in a hydrogen plasma. This line agrees well with hydrogen located in the $BC_\parallel$ position.[9] A different O–H vibrational line at 3326 cm^{-1} was discovered by McCluskey *et al.*[10] for ZnO samples annealed in H_2 gas at elevated temperature. This line was assigned to an O–H center with a transition moment oriented at an angle of 112° with respect to the c axis.[11]

(ii) *Hydrogen attached to defects*, there is a number of experimental results coming, e.g., from IR spectroscopy[8,9] and Raman spectroscopy,[12] which give evidence for hydrogen-related defects in ZnO crystals. Theoretical calculations[6,13] showed that hydrogen can be trapped at an oxygen vacancy (V_O). Recently, Janotti and Van de Walle[14] suggested that hydrogen forms a new type of strong multicenter bond in V_O. However, no clear experimental evidence of hydrogen trapped at V_O has been obtained so far. Regarding the zinc vacancy (V_{Zn}), certain lines ob-

---

a)Electronic mail: jakub.cizek@mff.cuni.cz.

served in IR spectra were attributed to two hydrogen atoms bound to V_{Zn}.[8,9]

(iii) *Loose (unbound) hydrogen*, it was suggested that the H-vibrational line at 3326.3 cm^{-1} can be produced by H_2 molecules.[15] This loose hydrogen is situated in "open channels" parallel with the *c* axis.

Apart of the hydrogen present *unintentionally* in the as-grown crystals, it is possible to introduce hydrogen into a ZnO crystal *intentionally* in order to modify its properties. An increase of the hydrogen concentration in ZnO up to 10^{18} cm^{-3} (0.003 at. %) was achieved using plasma charging.[16] A similar increase of the hydrogen concentration was obtained by high temperature exposition to H_2 gas.[17] However, recent extended nuclear reaction analysis (NRA) investigations of the hydrogen content in HTG ZnO crystals[7] have shown that these concentrations reported[16,17] are about two orders of magnitude smaller than the hydrogen amount being present already in the virgin crystals. Interestingly, it was reported[15] that hydrogen is commonly present in as-grown ZnO crystals in a form that is "hidden" from IR spectroscopy. Due to hidden hydrogen, the actual hydrogen content in the as-grown and H_2 gas treated specimens may be significantly higher than that determined from combined local mode free-carrier absorption and Hall measurements.[15] Recently, it was demonstrated[18] that hydrogen loading of ZnO can be performed electrochemically. The authors used ZnO powder mixed with "Nafion" as a proton conductor. However, the hydrogen concentration finally introduced into ZnO by electrochemical loading was not determined. Electrochemical hydrogen charging of ZnO single crystals has not been reported so far to the authors' best knowledge.

Positron annihilation spectroscopy (PAS) is a well established technique with a very high sensitivity to open volume defects.[19] Two complementary PAS techniques are very useful to study open volume defects: (a) positron lifetime (LT) spectroscopy,[20] which in principle enables us to identify the type of defects and to determine defect densities, and (b) coincidence Doppler broadening (CDB),[21] which carries information about the local chemical environment of defects.

Several PAS studies of ZnO crystals have been reported so far.[22–29] Unfortunately, the hydrogen content in the studied crystals was unknown in all these works. From the obtained results, one can conclude that the ZnO bulk lifetime lies in the range of $\tau_B = 151–159$ ps, which agrees well with the state-of-art theoretical calculations.[28]

Regarding intrinsic defects in ZnO, the calculations[13,28] have shown that V_O is too shallow to trap positrons at room temperature. On the other hand, V_{Zn} is a deep trap characterized by a calculated positron lifetime of $\tau_{V\text{-}Zn} = 194–229$ ps.[28] However, experimental LT values falling into this range were observed experimentally only in electron irradiated ZnO.[25,26,30]

As-grown ZnO crystals always exhibit a shorter lifetime lying somewhere between τ_B and $\tau_{V\text{-}Zn}$. In Ref. 30, it was shown that these observed lifetimes fall into four well separated groups and it was suggested that shortening of positron lifetime with respect to $\tau_{V\text{-}Zn}$ might be due to a various num-

ber of hydrogen atoms attached to V_{Zn}. Theoretical modeling of hydrogen attached to V_{Zn} (Ref. 30) supports this hypothesis.

CDB studies of ZnO crystals are much rarer so far. The authors in Ref. 29 used CDB to compare their virgin ZnO with the crystal state after electron irradiation. However, they made no attempt to characterize local chemical surrounding of positron annihilation sites in their virgin ZnO.

In the present work, it will be shown that ZnO crystals can be electrochemically doped with hydrogen. The amount of hydrogen introduced electrochemically is determined by NRA.[31] This technique has already been successfully used for the determination of hydrogen content, e.g., at HTG ZnO crystals[7] and nanorods.[32] NRA determines the overall hydrogen concentration in the specimen and even may reveal if the hydrogen is either in loose form or chemically bound, while PAS is sensitive almost exclusively to hydrogen attached to open volume defects.

II. EXPERIMENTAL

A. Sample preparation

HTG (0001) oriented ZnO single crystals (MaTecK GmbH) with O-terminated surface were studied. Each specimen (dimensions of $10 \times 10 \times 0.5$ mm^3) has one side optically polished, while the opposite one was unpolished.

The polished side was covered by a 20 nm thick Pd overlayer deposited by a cold cathode beam sputtering performed in an UHV chamber (base pressure of 10^{-10} mbar) at room temperature. The Pd overlayer acts as a catalyst for hydrogen permeation into ZnO and prevents hydrogen losses due to the formation of H_2 molecules on the surface.[33]

B. Hydrogen loading

The specimens were electrochemically doped with hydrogen[33] in a cell filled with a 1:1 mixture of H_3PO_4 and glycerin. The electrochemical hydrogen charging was performed by constant current pulses (current density *i* $=0.3$ mA cm^{-2}) using a Pt counterelectrode, while the loaded specimen was acting as cathode. Assuming no hydrogen losses (i.e., all transported protons are absorbed in the loaded sample), the hydrogen concentration, c_H, introduced into the specimen can be easily calculated from Faraday's law. The electrochemical hydrogen potential (emf) of the specimen with respect to a reference Ag/AgCl electrode was recorded during loading.

The hydrogen content was determined also by standard NRA using the resonant nuclear reaction $^{15}N + {}^{1}H \rightarrow {}^{12}C + {}^{4}He + \gamma$ rays.[31] Thereby, the hydrogen concentration can be calculated from the measured yield of the 4.43 MeV γ rays,[34] and a detection limit of 0.02 at. % was reached. The hydrogen concentration was determined at a sample depth of ~ 100 nm, as estimated by SRIM calculations.[35]

C. PAS

A ^{22}NaCl positron source (~ 1.5 MBq) deposited on a 2 μm thick Mylar foil was used in LT and CDB measurements. This source was always forming a sandwich with two

TABLE I. The results obtained by LT spectroscopy, NRA, and XRD on the ZnO crystals. The symbol τ_1 denotes lifetime values resolved in the LT spectrum, "c_H bound" and "c_H loose" are the concentrations of bound and loose hydrogen, respectively, obtained by NRA, while "c_H calc." denotes the net hydrogen concentration introduced into the specimen calculated from Faraday's law. The lattice parameters determined by XRD are given in the last two columns. The errors (one standard deviation) are shown in parentheses.

Sample	τ_1 (ps)	c_H bound (at. %)	c_H loose (at. %)	c_H calc. (at. %)	a (Å)	c (Å)
Virgin	181.9(3)[a] 181.6(3)[b]	0.3(1)[a]	<0.1[a]	⋯	n.a.	n.a.
After Pd cap sputtering	182.0(2)[a]	n.a.	n.a.	⋯	3.249 42(5)[a]	5.207 35(2)[a]
Loaded 3.4 h	179.6(2)[a]	n.a.	n.a.	3.5[a]	n.a.	n.a.
Loaded 24.5 h	178.8(4)[a] 178.9(3)[b]	20.6(1)[a] 12.4(1)[b]	23.7(1)[a] 4.8(1)[b]	25.0[a]	3.249 7(3)[a] 3.249 6(3)[b]	5.207 0(1)[a] 5.207 0(1)[b]

[a]The data measured on the polished crystal side covered subsequently with Pd layer.
[b]The data measured on the opposite crystal side.

identically treated ZnO crystals. In order to examine the uniformity of hydrogen-induced changes in the specimen, measurements are generally performed on both sides of specimens. This means that either the polished or the unpolished side of each crystal was facing the positron source during the measurement.

The source contribution in LT spectra consists of two weak components with lifetimes of ~368 ps and ~1.5 ns and corresponding intensities of ~8% and ~1%. The positron implantation profile of energetic positrons emitted by ^{22}Na is exponential[20]

$$P(x) = \alpha \exp(-\alpha x), \quad \alpha \approx 16 \frac{\rho(\text{g cm}^{-3})}{E_{\max}^{1.4}(\text{MeV})} \text{ cm}^{-1}, \quad (1)$$

where ρ is the density of the solid under investigation and $E_{\max}=0.54$ MeV is the maximum energy of positrons emitted by the ^{22}Na source. Using a ZnO density of 5.605 g cm^{-3}, a characteristic penetration depth into ZnO, $\alpha^{-1}=48$ μm, can be calculated. Integrating the expression given in Eq. (1) yields the fraction F of positrons which are stopped in the specimen somewhere between the surface and a depth x,

$$F(x) = 1 - \exp(-\alpha x). \quad (2)$$

Using Eq. (2), it can be deduced that ~90% of positrons annihilate in the depth up to 100 μm from surface (i.e., 1/5 of the sample thickness).

LT spectroscopy was performed using a fast-fast spectrometer[36] with timing resolution of 160 ps (full width at half maximum ^{22}Na). At least 10^7 positron annihilation events were accumulated at each LT spectrum which was subsequently decomposed using a maximum likelihood procedure.[37]

CDB studies were carried out on a spectrometer[38] equipped with two high purity Ge detectors. The energy resolution of the CDB spectrometer was 1.02 keV at 511 keV. At least 10^8 annihilation events were collected in each two dimensional γ-ray energy spectrum.

D. XRD

The x-ray diffraction (XRD) measurements were performed on an X'Pert high-resolution diffractometer

(PanAnalytical) using Cu $K\alpha$ radiation. The primary beam was conditioned by means of an x-ray mirror and Bartel's monochromator $4 \times$ Ge220. Channel-cut analyzator $3 \times$ Ge220 was placed in the diffracted beam.

E. Microscopies at the sample surface

The surface of the specimens was examined by a metallographic optical microscope (OM) Arsenal AM-2T.

III. EXPERIMENTAL RESULTS AND DISCUSSION

A. PAS

Results of LT measurements, NRA, and XRD are collected in Table I. It can be seen that the crystals contain an impressively high amount of hydrogen already in their virgin state. About 27% of the hydrogen is tightly bound in the ZnO lattice. It should be mentioned that the concentration of bound hydrogen already present in the virgin crystal, i.e., 0.3 at. % (~2.5×10^{20} cm^{-3}), is two orders of magnitude higher than that estimated to be introduced by plasma treatment of high temperature exposure to H$_2$ gas.[17]

The virgin crystal pair exhibits a single component LT spectrum with a lifetime of 182 ps. No difference between measurements of the polished and the unpolished side facing the positron source was detected on the virgin crystals. This lifetime measured is significantly longer than the supposed to be bulk ZnO lifetime $\tau_B = 151-159$ ps. It indicates that virtually, all positrons are trapped at defects (saturated positron trapping).

On the other hand, it is also remarkably smaller than $\tau_{V\text{-}Zn}$, testifying that positron traps are smaller than V_{Zn}. As V_O is unable to trap positrons,[13,28] a natural explanation of the observed lifetime is that positrons are trapped at V_{Zn} surrounded by hydrogen atoms which cause shortening of positron lifetime with respect to $\tau_{V\text{-}Zn}$. A detailed discussion of the nature of positron trapping sites in HTG ZnO crystals is given in Ref. 7. It is worth mentioning that HTG ZnO crystals from various suppliers all exhibit a positron lifetime falling into a narrow interval of 180–182 ps only. At the same time, it was found that all these crystals contain a significant amount of chemically bound hydrogen (0.3–0.8 at. %).[7] It leads to an unavoidable conclusion that
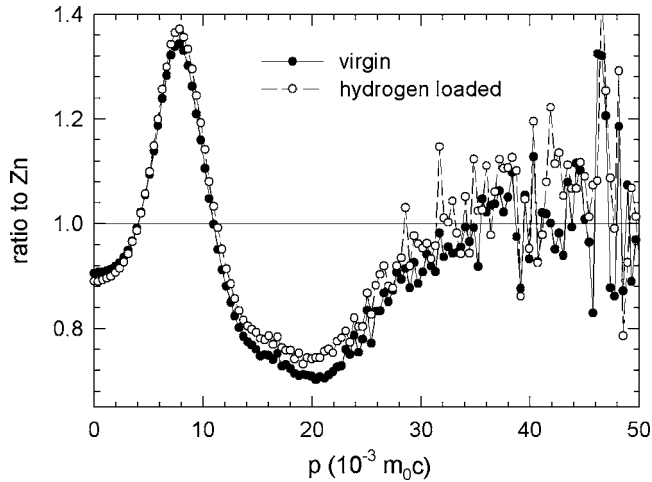
FIG. 1. CDB ratio curves related to pure well annealed Zn. The full circles show the curve for a virgin ZnO crystal, while the curve measured on ZnO loaded with hydrogen for 24.5 h (Pd cap side) is plotted by open circles.
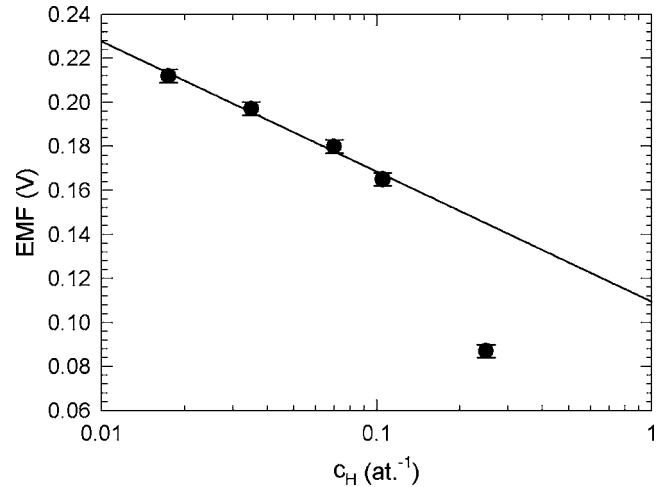

FIG. 2. The equilibrium emf potential measured on the electrochemically charged ZnO crystal. Note that the solid line plotted in the figure has slope $kT/e \ln(10)$ because the concentration of hydrogen on the x axis is in common logarithm scale.

positrons in HTG ZnO crystals are trapped at V_{Zn} surrounded with hydrogen atoms. This picture is supported also by the state-of-the-art theoretical calculations performed in Ref. 7. From the sensitivity of LT spectroscopy and using the specific trapping coefficient $(3 \times 10^{15} \text{ s}^{-1})$ given in Ref. 26, one can estimate that the V_{Zn} concentration is at least ~ 7 ppm $(6 \times 10^{17} \text{ cm}^{-3})$.

Figure 1 shows the CDB ratio curve measured on the virgin ZnO crystal. This curve is related to a well annealed, pure (99.99%) Zn specimen. The latter represents, thereby, 100% positron annihilations with Zn electrons. A sharp peak at $p \sim (8 \times 10^{-3}) m_0 c$ seen in the CDB curve measured on the ZnO crystal is due to positron annihilations with $2p$ O electrons, while a minimum at $p \sim (20 \times 10^{-3}) m_0 c$ is due to annihilations with $3d$ Zn electrons which are absent in an O atom.

B. XRD

The lattice parameters obtained by XRD are in agreement with those determined in Ref. 39. A systematic investigation of the c lattice parameter on HTG (0001) ZnO crystals from various producers was performed in Ref. 7. It was found that there is a scattering of the c parameter among crystals of various suppliers indicating slight lattice distortions due to both a variable (but always rather high) hydrogen content and also a variety of other impurities.[7]

C. Hydrogen loading

The cathodic process taking place at the charged ZnO crystal surface can be schematized as follows:[18]

$$H^+ + e^-(\text{ZnO}) = H_{\text{ZnO}}. \qquad (3)$$

Assuming an ideal hydrogen solution in ZnO, the emf potential of the doped specimen is proportional to the natural logarithm of the hydrogen concentration,

$$\text{emf} \sim -kT/e \ln(c_H). \qquad (4)$$

Figure 2 shows the equilibrium emf potential values as a function of the logarithm of hydrogen concentration. At lower hydrogen concentrations, the points fall into a straight line with a slope of 25.8 ± 0.3 mV which corresponds well with the theoretical value for a single electron process $kT/e = 25.69$ mV at 298 K. The deviation from this behavior seen at $c_H \sim 25$ at. % is due to the effect of hydrogen-hydrogen interaction.[40]

The hydrogen content in the loaded samples as determined by NRA after the last loading step is shown in Table I. Clearly, the NRA results confirm that a high amount of hydrogen was introduced into the specimens by electrochemical loading. Interestingly, more than 50% of the introduced hydrogen is found to be chemically bound (i.e., incorporated into the ZnO lattice). It is reasonable to assume that the bound hydrogen is located predominantly in the lower energy BC positions,[6,8] while the loose hydrogen is likely located in the open channels along the c axis most probably in a form of H_2 molecules.[15] The NRA analysis was performed on both sides of the loaded ZnO sample (at depth of ~ 100 nm from surface). It turned out that the hydrogen concentration is not uniform in the sample cross section. The hydrogen content is substantially higher at the side covered with Pd cap where hydrogen was introduced into the crystal. The mean hydrogen concentrations obtained as averages of the values measured on both sides of the sample are 16.5 and 14.3 at. % for bound and loose hydrogen, respectively. Subtracting the concentration of bound hydrogen present already in the virgin sample, one obtains that *on average* 16.2 and 14.3 at. % of bound and loose hydrogen, respectively, were introduced into the crystal by electrochemical hydrogen loading. Hence, the net hydrogen concentration introduced on average into the crystal amounts to 30.5 at. % (2.5 $\times 10^{22} \text{ cm}^{-3}$) which is in reasonable agreement with the concentration of 25 at. % calculated from Faraday's law. Thus, it can be concluded that electrochemical charging enables us to introduce a very high amount of hydrogen into ZnO. It should be mentioned that a comparable hydrogen concentration of ~ 34 at. % was reported to be absorbed in ZnO nanowires loaded at room temperature with H_2 gas pressure in-

creased up to 60 bar,[41] but such a high concentration of hydrogen has never been observed in bulk ZnO crystals so far.

From first principles calculations, it was found that the activation energy for diffusion of interstitial hydrogen through BC and antibonded (AB) sites is 0.5 ± 0.1 eV.[42] Even much lower activation energy of 0.17 eV was measured for diffusion of interstitial deuterium.[43] Thus, interstitial hydrogen becomes certainly mobile already below room temperature. The concentration gradient of the bound hydrogen detected in the loaded ZnO crystal indicates, therefore, that a significant fraction of hydrogen is trapped at defects and cannot diffuse through BC and AB interstitial sites. This conclusion is in agreement with the reported thermal stability of IR lines corresponding to hydrogen-related defects.[8,11,44] NRA performed on the crystal side opposite that with the Pd cap revealed ~12 at. % of chemically bound hydrogen, and it is the concentration of the interstitial hydrogen bound in the BC positions. The excess of ~8 at. % H in addition to the ~12 at. % H (back side) found on the side with the Pd cap comes likely from hydrogen trapped at defects. Note that recent investigations[45] of the deuterium concentration profile in ZnO crystals, deuterized by plasma treatment, revealed a buildup of deuterium in an ~1 μm thick subsurface layer. From diffusion measurements, it was concluded that this is due to deuterium trapped at defects.[45]

According to recent first principles calculations,[14] hydrogen can be trapped at V_O and may form multicenter bonds with the surrounding Zn atoms. The V_O is, however, invisible for positrons—which is in concordance with a very slight change of positron lifetime measured on the loaded specimens (see Table I). Positrons are trapped exclusively at V_{Zn} and, therefore, they are sensitive only to hydrogen attached to these defects. However, due to the relatively high concentration of hydrogen (0.3 at. %) found in the virgin specimen, existing V_{Zn} are already surrounded by hydrogen atoms, which are responsible for the observed shortening of the positron lifetime in the virgin crystal to 182 ps. Our LT results on the loaded crystals testify that an addition of further hydrogen atoms into the vicinity of V_{Zn} has only a minor influence on the observable positron lifetime.

The concentration of loose hydrogen on the crystal side bearing the Pd cap is estimated to be almost five times higher than on the opposite side. This difference is most probably due to hydrogen chemisorption on the Pd surface, which acts as a catalyst for hydrogen uptake.[33,46] Indeed, an enhanced hydrogen uptake and increased kinetic of hydrogen absorption were reported in Ref. 47 for ZnO sensors covered with Pd.

The CDB ratio curve measured on the crystal side with the Pd cap of the crystal loaded for 24.5 h is plotted in Fig. 1. One can see that hydrogen loading causes an increase of the peak at $p \sim (8 \times 10^{-3}) m_0 c$, while the minimum at $p \sim (20 \times 10^{-3}) m_0 c$ becomes shallower. Thus, hydrogen doped crystal exhibits an overall increase of positron annihilations with high momentum core electrons at the expense of annihilations with low momentum, i.e., $p < (5 \times 10^{-3}) m_0 c$, valence electrons. This increase can be explained by an increasing fraction of positrons annihilated by electrons belonging
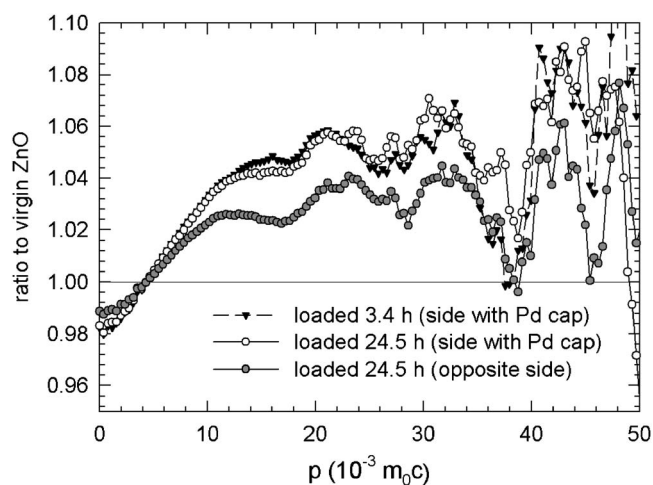

FIG. 3. CDB ratio curves (related to a virgin ZnO crystal) for ZnO crystals electrochemically doped with hydrogen. In order to reduce scattering, the curves were smoothed by Savitzky-Golay smoothing filter.

to O–H bonds. As the positrons are localized at V_{Zn}, they are sensitive only to hydrogen bound in the vicinity of V_{Zn}, e.g., hydrogen located at the BC positions adjacent to six nearest Zn atoms around the vacancy.

In order to examine exclusively the effect of hydrogen loading, CDB ratio curves measured on the hydrogen loaded crystals were related to the virgin ZnO, and results are plotted in Fig. 3. Obviously, hydrogen loading causes a broad peak in the high momentum range of $(5-38) \times 10^{-3} m_0 c$, which comes from positrons annihilated by electrons from O–H bonds. The CDB curves measured on the Pd cap side of the crystal loaded for 3.4 and 24.5 h are almost the same. It indicates that surrounding of V_{Zn} with hydrogen is saturated already after the first loading step and becomes essentially unchanged during further hydrogen loading. On the other hand, the CDB curve measured on the opposite side exhibits a remarkably lower contribution from O–H bonds. This is in agreement with a gradient in the concentration of bound hydrogen attributed to additional hydrogen trapped at defects.

The increased contribution of positron annihilations with electrons belonging to O–H bonds is well visible in the S-W plot commonly used to visualize the results of Doppler broadening measurements.[19] The S shape parameter is calculated as the central area of the annihilation peak (i.e., low momentum region) divided by the net peak area, while the W parameter is the area below the wings of the peak (i.e., high momentum regions) divided by the total peak area.[20] The regions for the shape parameters were chosen so that S_{Zn} is close to 0.5 and W_{Zn} close to 0.1 for the well annealed Zn specimen. All the shape parameters calculated from the CDB spectra were subsequently normalized to those for Zn. The normalized shape parameters S/S_{Zn} and W/W_{Zn} are plotted in Fig. 4. The virgin ZnO crystal should lie approximately on a line between the point for pure Zn and pure O. The S/S_{Zn} and W/W_{Zn} values for pure O are not available but should be located also on the dashed line shown in Fig. 4 if extended from the virgin ZnO point to the direction indicated by arrow, i.e., opposite the direction toward the Zn point. It is clearly seen in Fig. 4 that the points for hydrogen doped
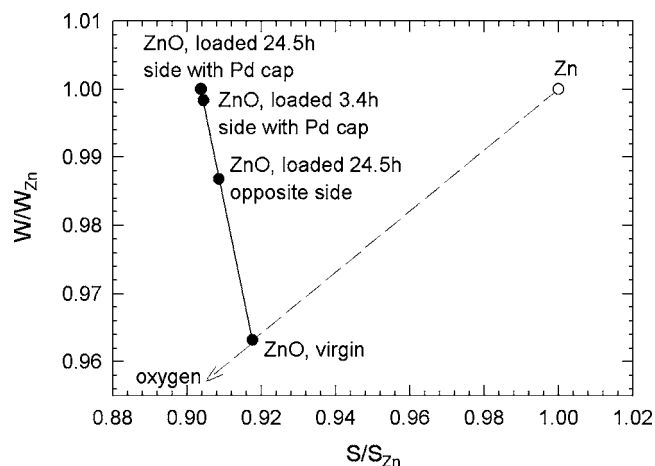
FIG. 4. *S-W* plot constructed from *S* and *W* parameters calculated from CDB spectra and normalized to those for the pure Zn specimen. The arrow indicates the direction where the point for pure O is expected to be located.

crystals are all located on a line going from the virgin crystal toward higher *W* and smaller *S* values, i.e., an enhanced contribution of annihilations with high momentum electrons. This line, however, points in a direction quite different from the direction toward the Zn, or the O, point. This gives evidence that there is a contribution of some kind of electrons, other than just O or Zn ones, which is gradually enhanced in the hydrogen doped specimens. We propose that this contribution comes from electrons belonging to O–H bonds formed by hydrogen being introduced into the crystals by electrochemical charging.

D. Microscopies at the sample surfaces

It has been observed that surfaces of the hydrogen loaded crystals were modified by hydrogen loading. These hydrogen-induced surface changes were investigated further by OM. Figure 5(a) shows a smooth surface of a virgin ZnO crystal covered with a Pd overlayer. The surface of the crystal doped with hydrogen for 24.5 h is shown in Fig. 5(b). A lot of hexagonal shape pyramids are visible at the surface of the loaded crystal. These pyramids have all the same orientation with respect to the crystal. Figure 5(c) shows these pyramids illuminated with cross light. It becomes clear from the figure that the pyramids grew out of the crystal. The side length of the pyramids is typically from 10 to 100 μm, and their height can be estimated to be several tens of microns. The pyramids appear already after hydrogen loading for 3.4 h, and they are found to be very similar at both sides of the crystal.

First principles calculations[6,8] have shown that hydrogen in BC positions causes a substantial outward relaxation of neighboring Zn and O atoms. Thus, incorporation of hydrogen into $BC_{\parallel}$ position causes a prolongation of the distance between the neighboring Zn and O atoms by $\sim$1 Å (in the [0001] direction).[6] Thus, hydrogen atoms located in $BC_{\parallel}$ positions should cause a lattice expansion in the [0001] direction, i.e., an increase of the *c*-lattice parameter. However, the lattice parameters measured on the loaded crystals by XRD (see Table I) are virtually the same as those obtained on the virgin crystals. This finding indicates that stresses caused by
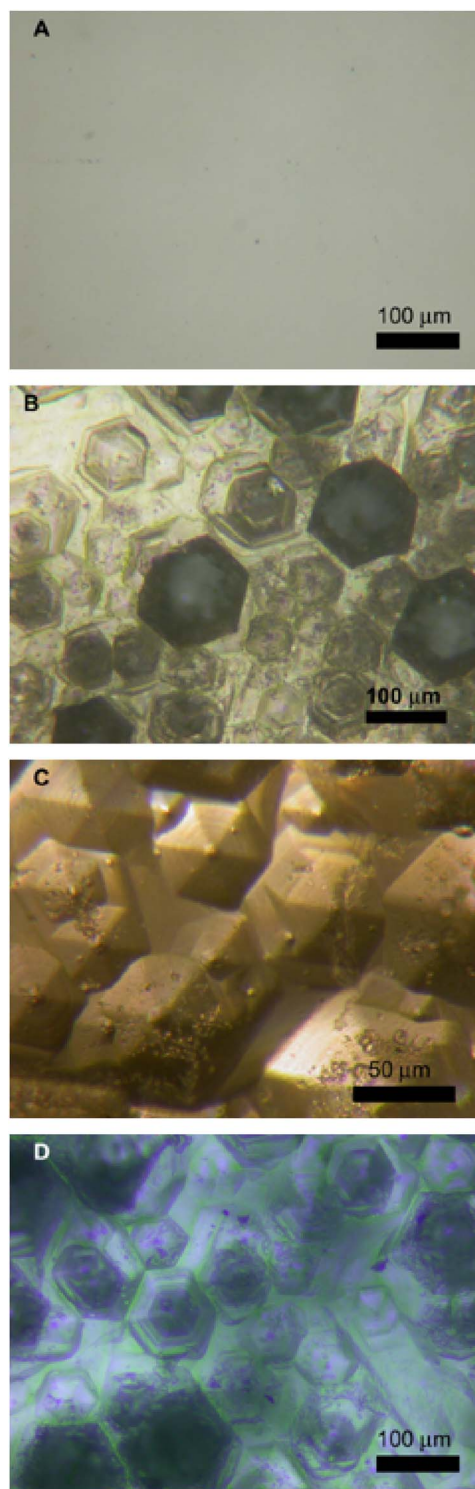

FIG. 5. (Color online) OM images of the ZnO crystal surface: (A) the virgin crystal covered with Pd overlayer (reflected light). [(B)–(D)] the crystal loaded for 24.5 h at various illuminating conditions: (B) reflected light, (C) cross light, and (D) UV light (in transmission).

hydrogen-induced lattice expansion were released by plastic deformation of the loaded crystal, which can be recognized through the hexagonal shape pyramids formed on the surface of the loaded crystals.

The following scenario is supposed: an increasing hydrogen concentration in the $BC_{\parallel}$ sites causes a lattice expansion in [0001] direction. At low hydrogen concentrations, this is still accumulated by elastic expansion. However, from

a certain critical hydrogen concentration, the hydrogen-induced stresses exceed the yield stress, and then plastic deformation occurs.

It was already shown that slip is a major mode of plastic deformation in ZnO.[48] Moreover, it is generally accepted that dislocations in crystals having a wurtzite structure have a primary slip on basal (0001) planes and a secondary slip on prismatic $\{1\bar{1}00\}$ planes.[49] The shape of the pyramids indicates that the plastic deformation occurs in the prismatic $\{1\bar{1}00\}$ slip planes. Terraces, which can be seen on the pyramids, support the picture that the pyramids were formed by a slip in the prismatic planes. The fact that deformation mainly occurs along the *c* axis supports the theoretical prediction[8] that the lowest energy sites for hydrogen are $BC_{\parallel}$ positions.

Furthermore, it was shown[50] that dislocations introduced by mechanical processing act as nonradiative recombination centers, thus lowering the overall luminescence efficiency. Figure 5(d) shows the pyramids illuminated by ultraviolet light. The well-known green luminescence (2.3 eV) observed frequently on ZnO crystals[23] is visible from the crystal bulk. However, the pyramids themselves appeared rather dark. This demonstrates that the green luminescence is quenched there due to an enhanced dislocation density. Note that similar dark band patterns, caused by an enhanced dislocation density, were observed on microscopic scale in cathode-luminescence microscopy studies of microhardness indentations in ZnO crystals.[51,52]

IV. CONCLUSIONS

HTG (0001) ZnO crystals contain already 0.3 at. % hydrogen in the virgin state. Thus, positrons are trapped at V_{Zn} surrounded by hydrogen atoms.

It was demonstrated that a high amount of hydrogen, namely, 30.5 at. %, can be introduced into such ZnO crystals by electrochemical charging. More than 50% of this concentration is chemically bound within the ZnO crystal lattice. Moreover, it was also found that even such a drastic increase of the hydrogen concentration has only a marginal impact on the positron lifetime. This result testifies too that positrons are trapped at V_{Zn} surrounded by hydrogen atoms present already in the virgin crystal.

The formation of O–H bonds in the vicinity of V_{Zn} was detected by CDB. It demonstrates that CDB is a very suitable technique for investigations of hydrogen-related defects in ZnO.

Furthermore, it was found that stresses caused by a hydrogen-induced lattice expansion are released by a slip in prismatic $\{1\bar{1}00\}$ planes. This leads to the formation of hexagonal shape pyramids on the surface of hydrogen-loaded crystals. The present results indicate also that ZnO could be a perspective material for hydrogen storage in future.

ACKNOWLEDGMENTS

[1] H. Cao, Y. G. Zhao, S. T. Ho, E. W. Seelig, Q. H. Wang, and R. P. H. Chang, Phys. Rev. Lett. **82**, 2278 (1999).

[2] K. Vanheusden, W. L. Warren, C. H. Seager, D. R. Tallant, J. A. Voight, and B. E. Gnade, J. Appl. Phys. **79**, 7983 (1996).

[3] T. K. Gupta, J. Am. Ceram. Soc. **73**, 1817 (1990).

[4] F.-C. Lin, Y. Takao, Y. Shimizu, and M. Egashira, J. Am. Ceram. Soc. **78**, 2301 (1995).

[5] D. C. Look, D. C. Reynolds, J. R. Sizelove, R. L. Jones, C. W. Litton, G. Cantwell, and W. C. Harsch, Solid State Commun. **105**, 399 (1998).

[6] C. G. Van de Walle, Phys. Rev. Lett. **85**, 1012 (2000).

[7] G. Brauer, W. Anwand, D. Grambole, J. Grenzer, W. Skorupa, J. Čížek, J. Kuriplach, I. Procházka, C. C. Ling, C. K. So, D. Schultz, and D. Klimm, "Evidence for a Zn vacancy — hydrogen complex in hydrothermally grown ZnO," Phys. Rev. Lett. (submitted).

[8] E. V. Lavrov, J. Weber, F. Börrnert, C. G. Van de Walle, and R. Helbig, Phys. Rev. B **66**, 165205 (2002).

[9] E. V. Lavrov, Physica B **340–342**, 195 (2003).

[10] M. D. McCluskey, S. J. Jokela, K. K. Zhuravlev, P. J. Simpson, and K. G. Lynn, Appl. Phys. Lett. **81**, 3807 (2002).

[11] S. J. Jokela, M. D. McCluskey, and K. G. Lynn, Physica B **340**, 221 (2003).

[12] N. H. Nickel and K. Fleicher, Phys. Rev. Lett. **90**, 197402 (2003).

[13] H. Takenaka and D. J. Singh, Phys. Rev. B **75**, 241102(R) (2007).

[14] A. Janotti and C. G. Van de Walle, Nat. Mater. **6**, 44 (2007).

[15] G. A. Shi, M. Saboktakin, M. Stavolaa, and S. J. Pearton, Appl. Phys. Lett. **85**, 5601 (2004).

[16] N. Ohashi, T. Ishigaki, N. Okada, H. Taguchi, I. Sakaguchi, S. Hishita, T. Sekiguchi, and H. Haneda, J. Appl. Phys. **93**, 6386 (2003).

[17] C. H. Seager and S. M. Myers, J. Appl. Phys. **94**, 2888 (2003).

[18] C. Chianella, R. Palombari, and A. Petricca, Electrochim. Acta **52**, 369 (2006).

[19] R. Krause–Rehberg and H. Leipner, *Positrons Annihilation in Semiconductors: Defect Studies* (Springer, Berlin, 1999), Vol. 127.

[20] P. Hautojärvi and C. Corbel, *Proceedings of the International School of Physics "Enrico Fermi," Course CXXV*, edited by A. Dupasquier and A. P. Mills (IOS, Varena 1995), p. 491.

[21] K. G. Lynn, J. E. Dickman, W. L. Brown, M. F. Robbins, and E. Bonderup, Phys. Rev. B **20**, 3566 (1979).

[22] R. M. de la Cruz, R. Pareja, R. Gonzáles, L. A. Boatner, and Y. Chen, Phys. Rev. B **45**, 6581 (1992).

[23] M. Liu, A. H. Kitai, and P. Mascher, J. Lumin. **54**, 35 (1992).

[24] Z. Q. Chen, S. Yamamoto, M. Maekawa, A. Kawasuso, X. L. Yuan, and T. Sekiguchi, J. Appl. Phys. **94**, 4807 (2003).

[25] F. Tuomisto, V. Ranki, K. Saarinen, and D. C. Look, Phys. Rev. Lett. **91**, 205502 (2003).

[26] F. Tuomisto, K. Saarinen, D. C. Look, and G. C. Farlow, Phys. Rev. B **72**, 085206 (2005).

[27] S. Dutta, S. Chattopadhyay, D. Jana, A. Banerjee, S. Manik, S. K. Pradhan, M. Sutradhar, and A. Sarkar, J. Appl. Phys. **100**, 114328 (2006).

[28] G. Brauer, W. Anwand, W. Skorupa, J. Kuriplach, O. Melikhova, C. Moisson, H. von Wenckstern, H. Schmidt, M. Lorenz, and M. Grundmann, Phys. Rev. B **74**, 045208 (2006).

[29] Z. Q. Chen, S. J. Wang, M. Maekawa, A. Kawasuso, H. Naramoto, X. L. Yuan, and T. Sekiguch, Phys. Rev. B **75**, 245206 (2007).

[30] G. Brauer, J. Kuriplach, J. Čížek, W. Anwand, O. Melikhova, I. Procházka, and W. Skorupa, Vacuum **81**, 1314 (2007).

[31] W. A. Lanford, *Handbook of Modern Ion Beam Materials Analysis*, edited by R. Tesmer and M. Nastasi (Materials Research Society, Pittsburgh, PA, 1995), p. 193.

[32] G. Brauer, W. Anwand, D. Grambole, W. Skorupa, Y. Hou, A. Andreev, C. Teichert, K. H. Tam, and A. B. Djurisic, Nanotechnology **18**, 195301 (2007).

[33] R. Kircheim, Prog. Mater. Sci. **32**, 261 (1988).

[34] W. Rudolph, C. Bauer, K. Brankoff, D. Grambole, R. Grötzschel, C. Heiser, and F. Herrmann, Nucl. Instrum. Methods Phys. Res. B **15**, 508 (1986).

[35] J. F. Ziegler, J. P. Biersack, and U. Littmark, *The Stopping and Range of Ions in Solids* (Pergamon, New York, 1985).

[36] F. Bečvář, J. Čížek, L. Lešták, I. Novotný, I. Procházka, and F. Šebesta, Nucl. Instrum. Methods Phys. Res. B **443**, 557 (2000).

[37] I. Procházka, I. Novotný, and F. Bečvář, Mater. Sci. Forum **255–257**, 772 (1997).

[38] J. Čížek, I. Procházka, B. Smola, I. Stulíková, R. Kužel, Z. Matěj, and V. Cherkaska, Phys. Status Solidi A **203**, 466 (2006).

[39]E. H. Kisi and M. M. Elcombe, Acta Crystallogr., Sect. C: Cryst. Struct. Commun. **45**, 1867 (1989).

[40]T. Mütschele and R. Kirchheim, Scr. Metall. **21**, 135 (1987).

[41]H. Pan, J. Luo, H. Sun, Y. Feng, C. Poh, and J. Lin, Nanotechnology **17**, 2963 (2006).

[42]M. G. Wardle, J. P. Goss, and P. R. Briddon, Phys. Rev. Lett. **96**, 205504 (2006).

[43]K. Ip, M. E. Overberg, Y. W. Heo, D. P. Nortgon, S. J. Pearton, C. E. Stutz, B. Luo, F. Ren, D. C. Look, and J. M. Zavada, Appl. Phys. Lett. **82**, 385 (2003).

[44]E. V. Lavrov, F. Börrnert, and J. Weber, Phys. Rev. B **71**, 035205 (2005).

[45]N. H. Nickel, Phys. Rev. B **73**, 195204 (2006).

[46]M. A. Pick, J. W. Davenport, M. Strongin, and G. J. Dienes, Phys. Rev. Lett. **43**, 286 (1979).

[47]B. Sam Kang, H. Wang, L. C. Tien, F. Ren, B. P. Gila, D. P. Norton, C. R. Abernathy, J. Lin, and S. J. Pearton, Sensors **6**, 643 (2006).

[48]S. O. Kucheyev, J. E. Bradby, J. S. Williams, C. Jagadishi, and M. V. Swain, Appl. Phys. Lett. **80**, 956 (2002).

[49]Yu. A. Osip'yany and I. S. Smirnova, Phys. Status Solidi **30**, 19 (1968).

[50]I. Yonenaga, S. Itoh, and T. Goto, Physica B **340–342**, 484 (2003).

[51]J. T. Czernuszka and N. Pratt, Philos. Mag. Lett. **61**, 83 (1990).

[52]Z. Takkouka, N. Brihia, K. Guergouria, and Y. Marfaing, Physica B **366**, 185 (2005).